

# Journal of Mechanics of Materials and Structures

**HIGHLY ACCURATE NONCOMPATIBLE GENERALIZED MIXED  
FINITE ELEMENT METHOD FOR 3D ELASTICITY PROBLEMS**

Guanghai Qing, Junhui Mao and Yanhong Liu

**Volume 12, No. 4**

**July 2017**





## HIGHLY ACCURATE NONCOMPATIBLE GENERALIZED MIXED FINITE ELEMENT METHOD FOR 3D ELASTICITY PROBLEMS

GUANGHUI QING, JUNHUI MAO AND YANHONG LIU

Based on the generalized H–R mixed variational principle, the simple compatible and noncompatible generalized mixed elements (CGME, NCGME) for 3D linear elasticity problems were derived by the  $C_0$  continuous polynomial shape functions used usually in the displacement methods. Two of main features of the generalized mixed finite element methods corresponding to the CGME and NCGME are that the coefficient matrix of system of equations are automatically symmetric and invertible. Without any extra techniques of the traditional mixed methods, the displacement and stress results can be obtained directly from the linear system of equations by introducing the stress and displacement boundary conditions simultaneously. The numerical examples show that the displacement and stress variables converge stably. The resulting stresses of NCGME have nearly the same accuracy as displacements and are certainly more accurate than the common noncompatible displacement finite element methods.

### 1. Introduction

It is well known that the finite element minimum potential energy principle leads, as its Euler–Lagrange (EL) equations, to not only equilibrium within the element but also interelement traction reciprocity. The equilibrium finite element methods are also straightforward applications of the minimum complementary energy principle. The finite element complementary energy principle leads, as its EL equations, to not only kinematic compatibility within each element but also interelement displacement compatibility.

The above requirements of interelement displacement continuity and traction reciprocity on the admissible displacement variables and stress variables (respectively) may not provide sufficient flexibility in the finite element solution of several problems in linear elasticity, such as plate bending, shells, multilayered composites, and problems with singularities found in fracture mechanics, among others [Pian 1964].

To gain this flexibility in application, one may relax the conditions of displacement continuity or traction reciprocity at interelement boundaries on the admissible displacement or stress fields, by introducing these as a posteriori constraints into the respective finite element variational principles. This is the underlying concept in the hybrid finite element methods [Pian 1964] (the hybrid methods, in essence, belong to the displacement methods [Tian and Pian 2011]) and the mixed finite element methods [Herrmann 1967; Dunham and Pister 1968]. The hybrid methods and mixed methods for the elasticity problem are mostly based on the mixed variational principle, which is a form of the Hellinger–Reissner (H–R) mixed variational principle [Reissner 1950]. Unlike the hybrid methods, where the element matrices are condensed into a stiffness matrix on the element level, in the mixed methods the element matrix is generally assembled to the global coefficient matrix by the usual superposition process. Consequently,

---

*Keywords:* H-R mixed variational principle, mixed element, generalized H-R mixed variational principle, compatible generalized mixed element, noncompatible generalized mixed element.

the mixed methods generally include two fields in the linear system of equations (e.g., displacement and stress fields for linear elasticity problems). The solution of resulting governing equations immediately also yields the static variables, which are of basic interest in the analysis and design of a structure.

It should be mentioned that the boundary nodal stresses obtained from the finite element analysis are inconsistent with the prescribed stresses in the displacement methods [Tian and Pian 2011]. The convergence rate of the displacement models for problems with large gradients of stresses is slow [Hoa and Feng 1998]. The equilibrium methods are rarely used in practical computation due to the difficulty of creating finite element spaces incorporating the necessary constraints. Thus the practical choice is usually between the displacement methods and the mixed methods.

The early and classical contributions for the mixed methods are reviewed in [Oden 1973; Atluri et al. 1983; Morley 1989; Arnold 1990]. More recent developments and extensions may be found in [Belytschko et al. 2013; Bonet and Wood 1997; Zienkiewicz and Taylor 2000; Arnold 2002; Arnold and Winther 2002; Adams and Cockburn 2005; Arnold et al. 2007; 2008; Gatica et al. 2008; Sinwel 2009; Qiu and Demkowicz 2010; 2011; Gopalakrishnan and Guzmán 2011; Hu et al. 2016].

One of the most prominent advantages of the mixed methods is the avoidance of using  $C_1$  elements for plate bending and other fourth-order problems. This is because the mixed functional for plate bending involves no more than two derivatives in any term and hence, after a suitable integration by parts, may be evaluated on the finite element spaces with merely continuous elements. The primal variational principles, however, require the use of  $C_1$  elements [Atluri et al. 1983; Arnold 1990]. Hence, the mixed methods are widely used in the linear and nonlinear applications of plate and shells for elasticity.

It is well known that for nearly incompressible and incompressible materials, finite element computations based on a standard displacement formulation fail due to the onset of the locking phenomenon. The traditional mixed formulations are a valid alternative to locking-affected methods, since they provide mathematical models capable of treating both compressible and incompressible linear elasticity problems under a unified framework [Atluri et al. 1983]. Of course, the mixed methods are also applied extensively for the numerical analysis of fluid mechanics problems.

The stability of the numerical results refers to the invertibility of the system matrix representing the discrete problem. Compared with the displacement methods, the mathematical properties of the mixed methods are not simple. If the same polynomial interpolation functions applied in the displacement methods are used to express the displacement and stress variables, the linear system of equations of mixed methods based on the H–R mixed variational principle is symmetric but possesses zeros on the diagonal. Thus, the coefficient matrix is usually indefinite and not invertible. The questions of convergence rate and stability of the traditional mixed models have attracted many mathematicians [Babuška et al. 1977; Oden and Reddy 1976; Talaslidis 1979].

Some representative researches on the mixed methods in recent years should be mentioned here. Arnold and Winther [2002] suggested some stable elements for a two-dimensional problem; the corresponding method in three-dimensional space was first characterized by Adams and Cockburn [2005]; and thorough analyses of the finite elements were provided in [Arnold et al. 2008]. The construction of these elements is not convenient for computer program, since they are of high polynomial order, which implies large costs even for the lowest-order scheme. A mixed finite element method was constructed by the tangential displacement-normal-normal-stress (TDNNS) formulation in [Sinwel 2009]. Thus, it is applicable for both nearly incompressible materials and the discretization of the thin structures using

flat elements. However, the mathematical theory and process on the basis of the TDNNS formulation are not simple and not suitable for engineers.

In a word, the above works show that it is not easy to construct a pair of finite elements for the displacement vector and the symmetric stress tensor which satisfy the stability Brezzi's conditions [1974]. There are still some open questions left in connection with the mixed methods for 2D and 3D problems.

## 2. Basic theory

**2.1. Governing equations.** Consider a body under static loading. The body occupies the volume  $V$ .  $S$  is the surface of body.  $S = S_u \cup S_\sigma$ , where  $S_u$  and  $S_\sigma$  are the segments of  $S$  where displacements and surface tractions are prescribed, respectively; the outward unit normal on  $S$  is denoted by  $\mathbf{n} \equiv \mathbf{n}_i$ . Let  $\nabla$  be the gradient operator in the undeformed body which, under the assumption of infinitesimal deformation, is indistinguishable from the deformed body.

We define the following: stress  $\boldsymbol{\sigma} \equiv \sigma_{ij}$  and strain  $\boldsymbol{\varepsilon} \equiv \varepsilon_{ij}$ ; the surface traction  $\mathbf{T} \equiv T_i$  and the prescribed surface traction  $\bar{\mathbf{T}} \equiv \bar{T}_i$  on  $S_\sigma$ ; the prescribed displacement  $\bar{\mathbf{u}} \equiv \bar{u}_i$  on  $S_u$ ; and  $\bar{\mathbf{b}} \equiv \bar{b}_i$  is the body force in  $V$ . Thus, the boundary value problems in linear elasticity can be stated as:

- The constitutive relations:

$$\boldsymbol{\sigma} = \mathbf{C}\boldsymbol{\varepsilon} \quad \text{or} \quad \sigma_{ij} = C_{ijkl}\varepsilon_{kl} \quad \text{or} \quad \boldsymbol{\varepsilon} = \mathbf{S}\boldsymbol{\sigma} \quad \text{in } V, \quad (1)$$

where  $\mathbf{C}$  is symmetric stiffness matrix of material and  $\mathbf{S} = \mathbf{C}^{-1}$  is compliance matrix.

- The strain-displacement equations (the compatible equations):

$$\boldsymbol{\varepsilon} = \nabla \mathbf{u} \quad \text{or} \quad \varepsilon_{ij} = \frac{1}{2}(u_{i,j} + u_{j,i}) \quad \text{in } V. \quad (2)$$

- The equilibrium equations:

$$\nabla^T \boldsymbol{\sigma} + \bar{\mathbf{b}} = 0 \quad \text{or} \quad \sigma_{ij,j} + \bar{b}_i = 0 \quad \text{in } V. \quad (3)$$

- The surface tractions boundary conditions:

$$\mathbf{n} \cdot \boldsymbol{\sigma} = \bar{\mathbf{T}} \quad \text{or} \quad \bar{T}_i = \sigma_{ij}n_j \quad \text{on } S_\sigma. \quad (4)$$

- The displacement boundary conditions:

$$\mathbf{u} = \bar{\mathbf{u}} \quad \text{or} \quad u_i = \bar{u}_i \quad \text{on } S_u. \quad (5)$$

**2.2. H–R mixed variational principle and generalized H–R mixed variational principle.** The H–R mixed variational principle contains the displacement field and stress field. Satisfying the displacement boundary conditions (5) a priori, such a principle takes the form

$$\Pi_{\text{HR}} = \int_V \left( -\frac{1}{2} \boldsymbol{\sigma}^T \mathbf{S} \boldsymbol{\sigma} + \boldsymbol{\sigma}^T (\nabla \mathbf{u}) - \bar{\mathbf{b}}^T \mathbf{u} \right) dV - \int_{S_\sigma} \bar{\mathbf{T}}^T \mathbf{u} dS. \quad (6)$$

Like the H–R mixed variational principle, there are also both displacement and stress fields in the generalized H–R mixed variational principle [Chien 1983]. This principle can be expressed as

$$\Pi_{\text{GHR}} = \Pi_{\text{HR}} + \int_V \lambda \left( \frac{1}{2} \boldsymbol{\sigma}^T \mathbf{S} \boldsymbol{\sigma} + \frac{1}{2} (\nabla \mathbf{u})^T \mathbf{C} (\nabla \mathbf{u}) - \boldsymbol{\sigma}^T (\nabla \mathbf{u}) \right) dV. \quad (7)$$

We should point out that Felippa [1989a; 1989b] constructed a one-parameter family of mixed variational principles for linear elasticity. This family includes the generalized H–R mixed and the minimum potential energy principles as special cases. We expect to take  $0 \leq \lambda \leq 1$  in (7). If the parameter  $\lambda < 0$  or  $\lambda > 1$ , there does not exist practical interest.

It is clear that, letting  $\lambda = 0$ , (7) is the H–R mixed variational principle, and letting  $\lambda = 1$  yields the minimum potential energy principle.

Letting  $\lambda = \frac{1}{2}$  leads to the simplest generalized H–R mixed variational principle:

$$\Pi_{\text{GHR}} = \int_V \left( -\frac{1}{4} \boldsymbol{\sigma}^T \mathbf{S} \boldsymbol{\sigma} + \frac{1}{2} \boldsymbol{\sigma}^T (\nabla \mathbf{u}) + \frac{1}{4} (\nabla \mathbf{u})^T \mathbf{C} (\nabla \mathbf{u}) - \bar{\mathbf{b}}^T \mathbf{u} \right) dV - \int_{S_\sigma} \bar{\mathbf{T}}^T \mathbf{u} dS. \quad (8)$$

For principles (6)–(8), the only constraint conditions are given in (1), while the equilibrium equations (3) and the traction boundary conditions (4) are satisfied a posteriori.

We assume that all equations in the following sections are for the same finite element model. For clarity, the matrices or vectors with the same symbol in the following imply the identical expressions.

### 3. Compatible and noncompatible generalized mixed finite element formulations

**3.1. Mixed finite element formulations based on H–R mixed variable principle.** Without loss of generality, consider an  $n$ -node compatible linear element for 3D linear elasticity problems. Both displacement  $\mathbf{u}$  and stress  $\boldsymbol{\sigma}$  are expressed by the same shape functions:

$$\mathbf{u} = N_q \mathbf{q}_e, \quad (9)$$

$$\boldsymbol{\sigma} = N_p \mathbf{p}_e. \quad (10)$$

Here,

$$\begin{aligned} \text{Diag}(N_q) &= [N_e, N_e, N_e]^T, \quad N_e = [N_1, N_2, \dots, N_n], \quad \mathbf{q}_e = [\mathbf{u}_{e1}, \mathbf{u}_{e2}, \mathbf{u}_{e3}]^T, \\ \text{Diag}(N_p) &= [N_e, N_e, N_e, N_e, N_e, N_e]^T, \quad \mathbf{p}_e = [\boldsymbol{\sigma}_{e13}, \boldsymbol{\sigma}_{e23}, \boldsymbol{\sigma}_{e33}, \boldsymbol{\sigma}_{e11}, \boldsymbol{\sigma}_{e22}, \boldsymbol{\sigma}_{e12}]^T. \end{aligned}$$

Let  $N_i = \frac{1}{8}(1 + \zeta_i \zeta)(1 + \eta_i \eta)(1 + \xi_i \xi)$ ,  $i = 1, 2, 3, \dots, 8$ , in (9) and (10); thus  $N_q$  and  $N_p$  are the 24 by 24 and 48 by 48 shape function matrices, respectively.

It is well known that by substituting (9) and (10) into (6) and performing the energy integration, one obtains the discrete functional

$$\Pi_{\text{HR}}(\mathbf{p}_e, \mathbf{q}_e) = \sum_{i=1}^n \left( -\frac{1}{2} \mathbf{p}_e^T \mathbf{K}_{\text{pp}}^{(i)} \mathbf{p}_e + \mathbf{p}_e^T \mathbf{K}_{\text{pq}}^{(i)} \mathbf{q}_e - (\mathbf{f}_q^{(i)})^T \mathbf{q}_e \right), \quad (11)$$

in which  $\sum$  implies summation with respect to all individual elements;  $\mathbf{K}_{\text{pp}}^{(i)} = \int_{V_i} N_p^T \mathbf{S} N_p dV$  is symmetric and positive definite matrix for each element;  $\mathbf{K}_{\text{pq}}^{(i)} = \int_{V_i} N_p^T (\nabla N_q) dV$  is a rectangular matrix; and  $\mathbf{f}_q^{(i)} = \int_{V_i} N_p^T \bar{\mathbf{b}} dV + \int_{S_{\sigma_i}} N_q^T \bar{\mathbf{T}} dS$  is the load vector of each element.

In the following, the superscript “(i)” of element submatrices will be dropped for clarity.

Consider  $\mathbf{p}_e$  and  $\mathbf{q}_e$  as independent variables. Using  $\delta\Pi_{\text{HR}}(\mathbf{p}_e, \mathbf{q}_e) = 0$  yields the two Euler–Lagrange (EL) equations

$$-\mathbf{K}_{pp}\mathbf{p}_e + \mathbf{K}_{pq}\mathbf{q}_e = 0, \tag{12a}$$

$$\mathbf{K}_{pq}^T\mathbf{p}_e = \mathbf{f}_q. \tag{12b}$$

The summation of (12a) and (12b) on all elements gives a linear system of equations with respect to both displacement and stress variables. It is well known as the mixed model:

$$\begin{bmatrix} -\mathbf{K}_{11} & \mathbf{K}_{12} \\ \mathbf{K}_{12}^T & \mathbf{0} \end{bmatrix} \begin{Bmatrix} \mathbf{p} \\ \mathbf{q} \end{Bmatrix} = \begin{Bmatrix} \mathbf{0} \\ \mathbf{f} \end{Bmatrix}. \tag{13}$$

Here, submatrices  $\mathbf{K}_{11} = \sum \mathbf{K}_{pp}$ ,  $\mathbf{K}_{12} = \sum \mathbf{K}_{pq}$ ; the vectors  $\mathbf{p} = \sum \mathbf{p}_e$ ,  $\mathbf{q} = \sum \mathbf{q}_e$ ; and the whole load vector  $\mathbf{f} = \sum \mathbf{f}_q$ .

The equation resulting from H–R mixed variational principles (6) of various physical problems is symmetric but possesses zeros on the diagonal. Indeed, it can be seen that the coefficient matrix of (13) is indefinite. For 2D or 3D problems, if the stable mixed element techniques [Adams and Cockburn 2005; Oden and Reddy 1976; Brezzi and Fortin 1991] are not employed, it is very difficult to obtain the stable and reliable solutions by (13).

**3.2. Compatible generalized mixed finite element formulations.** By the same way, using (9) and (10), the discrete form of the generalized H–R mixed variational principle is

$$\Pi_{\text{GHR}}(\mathbf{p}_e, \mathbf{q}_e) = \sum \left( -\frac{1}{4}\mathbf{p}_e^T \mathbf{K}_{pp} \mathbf{p}_e + \frac{1}{2}\mathbf{p}_e^T \mathbf{K}_{pq} \mathbf{q}_e + \frac{1}{4}\mathbf{q}_e^T \mathbf{K}_{qq} \mathbf{q}_e - \mathbf{f}_q^T \mathbf{q}_e \right). \tag{14}$$

In (14),  $\mathbf{K}_{qq} = \int_{V_e} (\nabla \mathbf{N}_q)^T \mathbf{C} (\nabla \mathbf{N}_q) dV$  is a full rank, symmetric, and positive definite matrix and undoubtedly it is equivalent to the expression derived from the minimum potential energy principle.

Similarly, the following 8-node compatible generalized mixed element (CGME) with 8 nodes for 3D problems can be derived from (14):

$$-\mathbf{K}_{pp}\mathbf{p}_e + \mathbf{K}_{pq}\mathbf{q}_e = 0, \tag{15a}$$

$$\mathbf{K}_{pq}^T\mathbf{p}_e + \mathbf{K}_{qq}\mathbf{q}_e = 2\mathbf{f}_q. \tag{15b}$$

It is of interest to see that (15) can also be obtained by combining the EL equations of the finite element potential energy principle and the finite element H–R mixed variational principle.

The summation of (15) on all elements gives a novel algebraic system

$$\begin{bmatrix} -\mathbf{K}_{11} & \mathbf{K}_{12} \\ \mathbf{K}_{12}^T & \mathbf{K}_{22} \end{bmatrix} \begin{Bmatrix} \mathbf{p} \\ \mathbf{q} \end{Bmatrix} = \begin{Bmatrix} \mathbf{0} \\ 2\mathbf{f} \end{Bmatrix}, \tag{16}$$

where  $\mathbf{K}_{11}$  and  $\mathbf{K}_{22}$  ( $= \sum \mathbf{K}_{qq}$ ) are symmetric and positive definite.

It is clear that the coefficient matrix of the above equation is indefinite because of submatrix  $-\mathbf{K}_{11}$ . However, it is characterized by symmetry and all elements on the leading diagonal are nonzero.

Comparing (16) and (13), the main difference is the values of elements on the diagonal.

**3.3. Noncompatible generalized mixed finite element formulations.** On the basis of [Chen 1982; Taylor et al. 1976], for a noncompatible element weak discontinuity, the element displacements can be expressed as a sum of the compatible part  $N_q \mathbf{q}_e$  and the noncompatible part  $N_r \mathbf{r}_e$ :

$$\mathbf{u} = N_q \mathbf{q}_e + N_r \mathbf{r}_e. \quad (17)$$

Here, the expression of  $N_r$  can be found in [Chen 1982];  $N_r$  are the shape functions with respect to points within elements;  $\mathbf{r}_e$  is the displacement vector corresponding to points within elements.

In a similar way, by (17) and (10), the finite element functional of the generalized mixed variational principle is given by

$$\begin{aligned} \Pi_{\text{GHR}}(\mathbf{p}_e, \mathbf{q}_e, \mathbf{r}_e) = \sum_{i=1}^n & \left( -\frac{1}{4} \mathbf{p}_e^T \mathbf{K}_{pp} \mathbf{p}_e + \frac{1}{2} \mathbf{p}_e^T \mathbf{K}_{pq} \mathbf{q}_e + \frac{1}{2} \mathbf{p}_e^T \mathbf{K}_{pr} \mathbf{r}_e + \frac{1}{4} \mathbf{q}_e^T \mathbf{K}_{qq} \mathbf{q}_e \right. \\ & \left. + \frac{1}{2} \mathbf{q}_e^T \mathbf{K}_{qr} \mathbf{r}_e + \frac{1}{4} \mathbf{r}_e^T \mathbf{K}_{rr} \mathbf{r}_e - \mathbf{f}_q^T \mathbf{q}_e - \mathbf{f}_r^T \mathbf{r}_e \right). \end{aligned} \quad (18)$$

In (18),

$$\begin{aligned} \mathbf{K}_{pr} = \mathbf{K}_{rp}^T &= \int_{V_i} N_p^T (\nabla N_r) dV, & \mathbf{K}_{qr} = \mathbf{K}_{rq}^T &= \int_{V_i} (\nabla N_q)^T \mathbf{C} (\nabla N_r) dV, \\ \mathbf{K}_{rr} = \mathbf{K}_{rr}^T &= \int_{V_i} (\nabla N_r)^T \mathbf{C} (\nabla N_r) dV, & \mathbf{f}_r &= \int_{V_i} N_r^T \bar{\mathbf{b}} dV + \int_{S_{\sigma_i}} N_r^T \bar{\mathbf{T}} dS. \end{aligned}$$

Taking the variation of (18) with respect to  $\mathbf{r}_e$  results in

$$\mathbf{K}_{rr} \mathbf{r}_e + \mathbf{K}_{pr}^T \mathbf{p}_e + \mathbf{K}_{qr}^T \mathbf{q}_e = 2 \mathbf{f}_r. \quad (19)$$

$\mathbf{K}_{rr}$  in the above equations is identical to the corresponding expression obtained from the minimum potential energy principle for noncompatible displacement elements [Chen 1982; Taylor et al. 1976], and  $\mathbf{K}_{rr}$  is an invertible matrix. Thus, one has

$$\mathbf{r}_e = 2 \mathbf{K}_{rr}^{-1} \mathbf{f}_r - \mathbf{K}_{rr}^{-1} \mathbf{K}_{pr}^T \mathbf{p}_e - \mathbf{K}_{rr}^{-1} \mathbf{K}_{qr}^T \mathbf{q}_e. \quad (20)$$

Finding the extrema of (18) with respect to  $\mathbf{p}_e$  and  $\mathbf{q}_e$  leads to two EL equations:

$$-\mathbf{K}_{pp} \mathbf{p}_e + \mathbf{K}_{pq} \mathbf{q}_e + \mathbf{K}_{pr} \mathbf{r}_e = 0, \quad (21)$$

$$\mathbf{K}_{pq}^T \mathbf{p}_e + \mathbf{K}_{qq} \mathbf{q}_e + \mathbf{K}_{pr}^T \mathbf{r}_e = 2 \mathbf{f}_q. \quad (22)$$

On substituting (20) into (21) and (22), one obtains

$$-\mathcal{K}_{pp} \mathbf{p}_e + \mathcal{K}_{pq} \mathbf{q}_e = -2 \mathbf{K}_{pr} \mathbf{K}_{rr}^{-1} \mathbf{f}_r, \quad (23a)$$

$$\mathcal{K}_{pq}^T \mathbf{p}_e + \mathcal{K}_{qq} \mathbf{q}_e = 2 \mathbf{f}_q - 2 \mathbf{K}_{qr} \mathbf{K}_{rr}^{-1} \mathbf{f}_r, \quad (23b)$$

in which

$$\mathcal{K}_{pp} = \mathbf{K}_{pp} + \mathbf{K}_{pr} \mathbf{K}_{rr}^{-1} \mathbf{K}_{pr}^T, \quad \mathcal{K}_{pq} = \mathbf{K}_{pq} - \mathbf{K}_{pr} \mathbf{K}_{rr}^{-1} \mathbf{K}_{qr}^T, \quad \mathcal{K}_{qq} = \mathbf{K}_{qq} - \mathbf{K}_{qr} \mathbf{K}_{rr}^{-1} \mathbf{K}_{qr}^T.$$

Note that, for general numerical examples, if the body force is ignored, the vectors  $2 \mathbf{K}_{pr} \mathbf{K}_{rr}^{-1} \mathbf{f}_r$  and  $2 \mathbf{K}_{qr} \mathbf{K}_{rr}^{-1} \mathbf{f}_r$  on the right-hand side of (21) are close to zero. Such a property is the same as the noncompatible displacement element formulations [Tian and Pian 2011]. Therefore, the following 8-node

noncompatible generalized mixed element (NCGME) problems is of the form

$$\begin{bmatrix} -\mathcal{K}_{pp} & \mathcal{K}_{pq} \\ \mathcal{K}_{pq}^T & \mathcal{K}_{qq} \end{bmatrix} \begin{Bmatrix} \mathbf{p}_e \\ \mathbf{q}_e \end{Bmatrix} = \begin{Bmatrix} \mathbf{0} \\ 2\mathbf{f}_q \end{Bmatrix}. \quad (24)$$

Similarly, the noncompatible generalized mixed model corresponding to (24) is as follows:

$$\begin{bmatrix} -\mathcal{K}_{11} & \mathcal{K}_{12} \\ \mathcal{K}_{12}^T & \mathcal{K}_{22} \end{bmatrix} \begin{Bmatrix} \mathbf{p} \\ \mathbf{q} \end{Bmatrix} = \begin{Bmatrix} \mathbf{0} \\ 2\mathbf{f} \end{Bmatrix}, \quad (25)$$

where submatrices  $\mathcal{K}_{11} = \sum \mathcal{K}_{pp}$ ,  $\mathcal{K}_{12} = \sum \mathcal{K}_{pq}$ ,  $\mathcal{K}_{22} = \sum \mathcal{K}_{qq}$ ; the vectors  $\mathbf{p} = \sum \mathbf{p}_e$ ,  $\mathbf{q} = \sum \mathbf{q}_e$ , and the whole load vector  $\mathbf{f} = \sum \mathbf{f}_q$ .

It is obvious that the main difference between (25) and (16) is their coefficient matrices.

**3.4. A unified approach for imposing stress and displacement boundary conditions.** Assume that symbol  $\mathbf{a}$  refers to the known value vector with respect to nodes on the surface or edges, whose values are determined by the prescribed surface traction  $\bar{\mathbf{T}}$  on  $S_\sigma$  and the prescribed displacement  $\bar{\mathbf{u}}$  on  $S_u$ .

Interchanging the rows and columns of (25), it can be recast into the form

$$\begin{bmatrix} -\hat{\mathcal{K}}_{11} & \hat{\mathcal{K}}_{12} & \hat{\mathcal{K}}_{13} \\ \hat{\mathcal{K}}_{12}^T & \hat{\mathcal{K}}_{22} & \hat{\mathcal{K}}_{23} \\ \hat{\mathcal{K}}_{13}^T & \hat{\mathcal{K}}_{23}^T & \hat{\mathcal{K}}_{33} \end{bmatrix} \begin{Bmatrix} \hat{\mathbf{p}} \\ \hat{\mathbf{q}} \\ \mathbf{a} \end{Bmatrix} = \begin{Bmatrix} \mathbf{f}_1 \\ \mathbf{f}_2 \\ \mathbf{f}_3 \end{Bmatrix}, \quad (26)$$

where  $\hat{\mathbf{p}}$  and  $\hat{\mathbf{q}}$  are the unknown parameter vectors of the nodal stresses and displacements, respectively.

Therefore,

$$-\hat{\mathcal{K}}_{11}\hat{\mathbf{p}} + \hat{\mathcal{K}}_{12}\hat{\mathbf{q}} = \mathbf{f}_1 - \hat{\mathcal{K}}_{13}\mathbf{a}, \quad (27a)$$

$$\hat{\mathcal{K}}_{12}^T\hat{\mathbf{p}} + \hat{\mathcal{K}}_{22}\hat{\mathbf{q}} = \mathbf{f}_2 - \hat{\mathcal{K}}_{23}\mathbf{a}, \quad (27b)$$

$$\hat{\mathcal{K}}_{13}^T\hat{\mathbf{p}} + \hat{\mathcal{K}}_{23}^T\hat{\mathbf{q}} = \mathbf{f}_3 - \hat{\mathcal{K}}_{33}\mathbf{a}. \quad (27c)$$

Of course, (27c) is redundant. Consequently, the final system of equations for the finite element solutions is

$$\begin{bmatrix} -\hat{\mathcal{K}}_{11} & \hat{\mathcal{K}}_{12} \\ \hat{\mathcal{K}}_{12}^T & \hat{\mathcal{K}}_{22} \end{bmatrix} \begin{Bmatrix} \hat{\mathbf{p}} \\ \hat{\mathbf{q}} \end{Bmatrix} = \begin{Bmatrix} \mathbf{f}_1 - \hat{\mathcal{K}}_{13}\mathbf{a} \\ \mathbf{f}_2 - \hat{\mathcal{K}}_{23}\mathbf{a} \end{Bmatrix}. \quad (28)$$

The above unified approach for imposing stress and displacement boundary conditions is employed in our program. In the next section, one of the numerical examples indicates that boundary nodal stresses are consistent with the prescribed stresses.

## 4. Numerical examples and discussions

**4.1. A thick rectangular plate with simply supported edges.** As shown in Figure 1, consider a thick rectangular plate with in-plane dimensions  $a = b = 1.0$  and thickness  $h = 0.10$ . The material properties are  $E_{11} = 10E_{22} = 10E_{33}$ ,  $G_{12} = G_{13} = 0.6E_{33}$ ,  $G_{23} = 0.5E_{33}$ , and  $\nu_{12} = \nu_{13} = \nu_{23} = 0.25$ . The boundary conditions are  $\sigma_{11} = u_2 = u_3 = 0$  on  $x_1 = 0$  and  $x_1 = a$ ; and  $\sigma_{22} = u_1 = u_3 = 0$  on  $x_2 = 0$  and  $x_2 = b$ . The uniform normal load 0.1 is on the upper surface of the plate [Fan 1996].

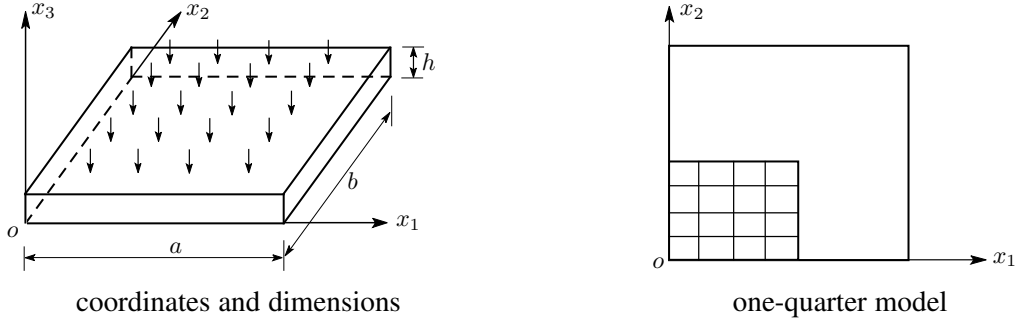


**Figure 1.** Coordinates and dimensions of a thick rectangular plate.

Using the symmetry about the  $x_1$  and  $x_2$ -axes, only one-quarter of plate (see Figure 1, right) is analyzed with uniform meshes. The convergence rate and accuracy of displacements and stresses at special locations are depicted in Figures 2–12. The notation  $l \times m \times n$  mesh denotes  $l$  subdivisions along the  $x_1$ -axis and  $m$  subdivisions along the  $x_2$ -axis with the same type of elements, while  $n$  denotes the element number in the  $x_3$  direction. The nodal stresses of the 8-node noncompatible displacement element (NCDE) for 3D problems in the commercially available software ABAQUS are obtained from the stresses of Gauss quadrature points by the extrapolation method. On the basis of the results of the  $12 \times 12 \times 4$  mesh, errors, which are illustrated in the legends in Figures 2–10, are computed by the formulation

$$\frac{\text{exact solution} - \text{solution of element}}{\text{exact solution}} \times 100\%.$$

In our computer program, two Gauss quadrature points in each direction are used for both CGME and NCGME.

As far as displacements  $u_1(\frac{1}{8}a, \frac{1}{2}b, h)$ ,  $u_2(\frac{1}{2}a, \frac{1}{8}b, h)$  and  $u_3(\frac{1}{2}a, \frac{1}{2}b, \frac{1}{2}h)$  are concerned (see Figures 2, 3, and 4), there is no significant difference between NCGME and NCDE for the convergence rate and accuracy. Certainly, it is clear that when the element mesh is relatively fine, the results of NCGME and NCDE are more accurate than those of CGME.

Figures 5 and 6 show that the results  $\sigma_{13}(\frac{1}{8}a, \frac{1}{2}b, \frac{1}{2}h)$  and  $\sigma_{23}(\frac{1}{2}a, \frac{1}{8}b, \frac{1}{2}h)$  of NCGME are in good agreement with the exact solution for even coarse meshes. It can also be observed that the accuracy of the  $\sigma_{13}(\frac{1}{8}a, \frac{1}{2}b, \frac{1}{2}h)$  and  $\sigma_{23}(\frac{1}{2}a, \frac{1}{8}b, \frac{1}{2}h)$  of the compatible element CGME are greatly superior to NCDE.

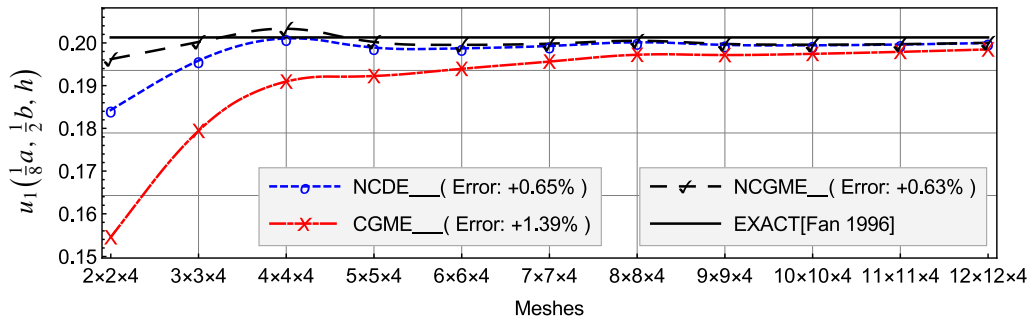


**Figure 2.** Comparison of displacement  $u_1(\frac{1}{8}a, \frac{1}{2}b, h)$ .

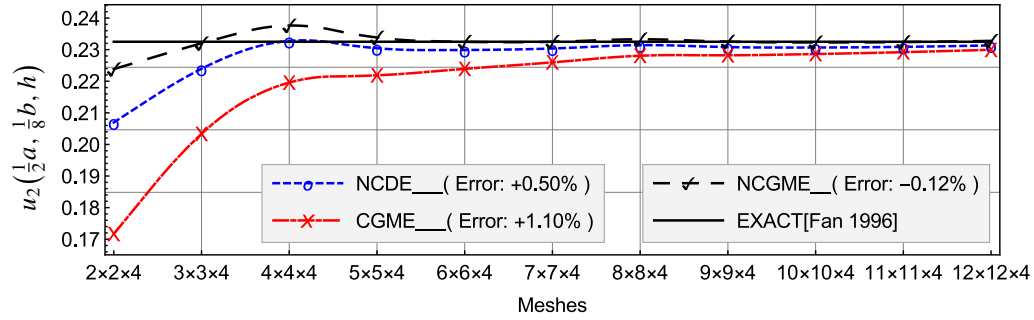


Figure 3. Comparison of displacement  $u_2(\frac{1}{2}a, \frac{1}{8}b, h)$ .

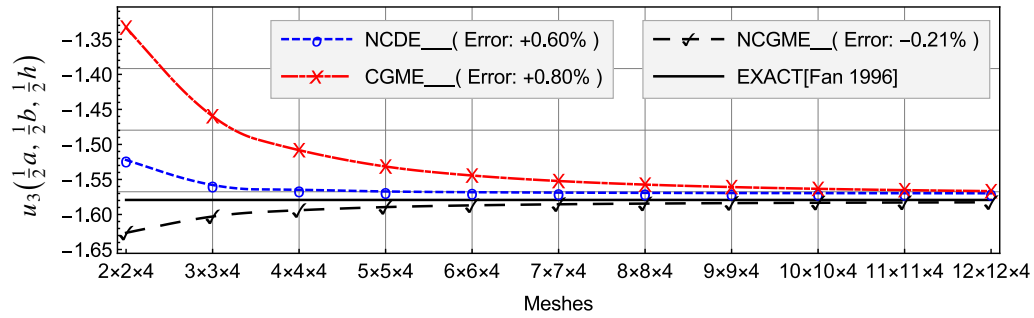


Figure 4. Comparison of displacement  $u_3(\frac{1}{2}a, \frac{1}{2}b, \frac{1}{2}h)$ .

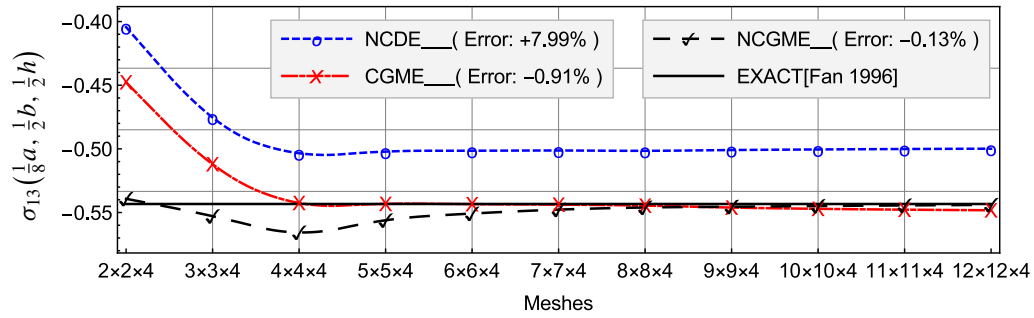


Figure 5. Comparison of stress  $\sigma_{13}(\frac{1}{8}a, \frac{1}{2}b, \frac{1}{2}h)$ .

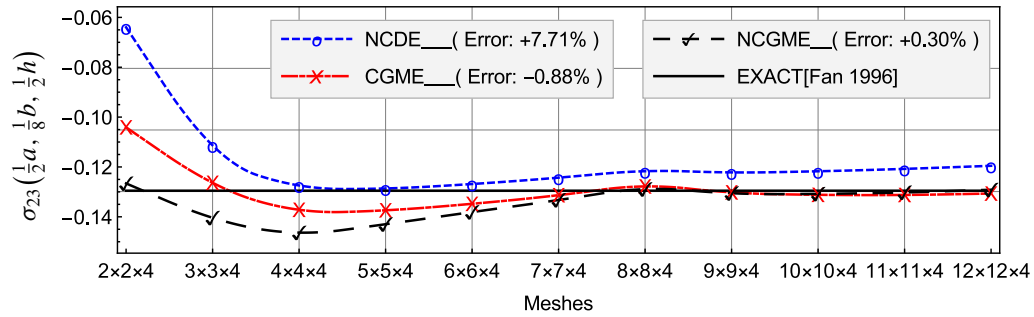


Figure 6. Comparison of stress  $\sigma_{23}(\frac{1}{2}a, \frac{1}{8}b, \frac{1}{2}h)$ .

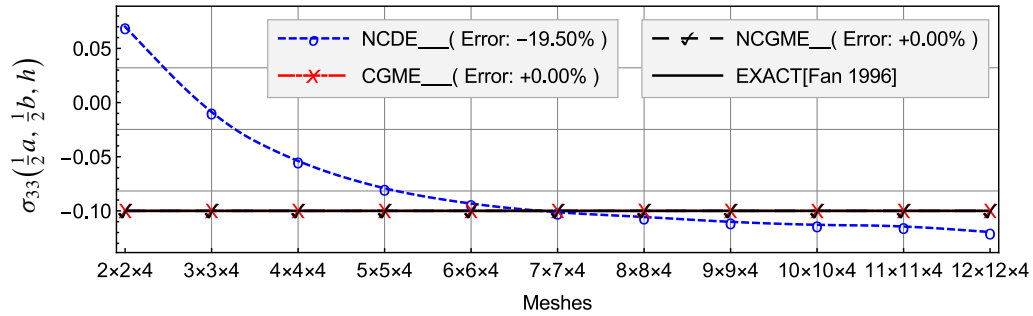


Figure 7. Comparison of stress  $\sigma_{33}(\frac{1}{2}a, \frac{1}{2}b, h)$ .

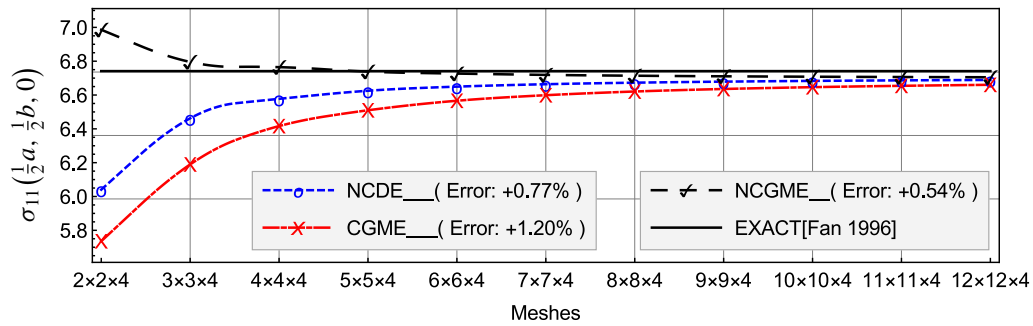


Figure 8. Comparison of stress  $\sigma_{11}(\frac{1}{2}a, \frac{1}{2}b, 0)$ .

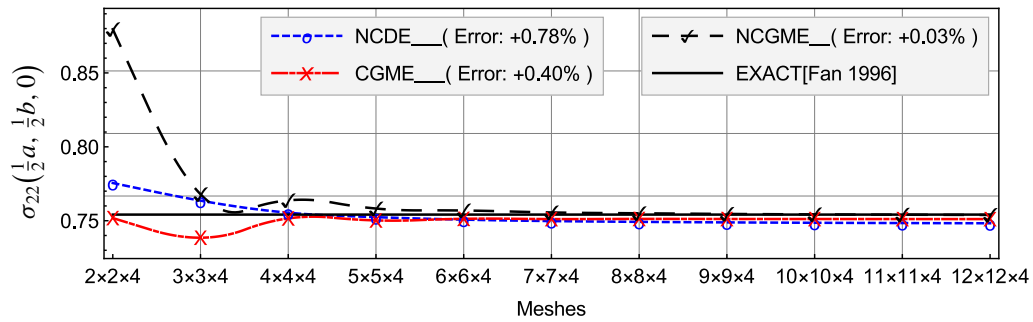


Figure 9. Comparison of stress  $\sigma_{22}(\frac{1}{2}a, \frac{1}{2}b, 0)$ .

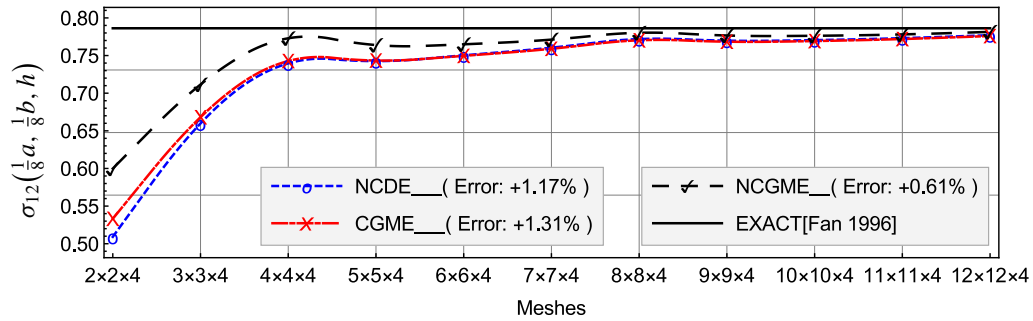
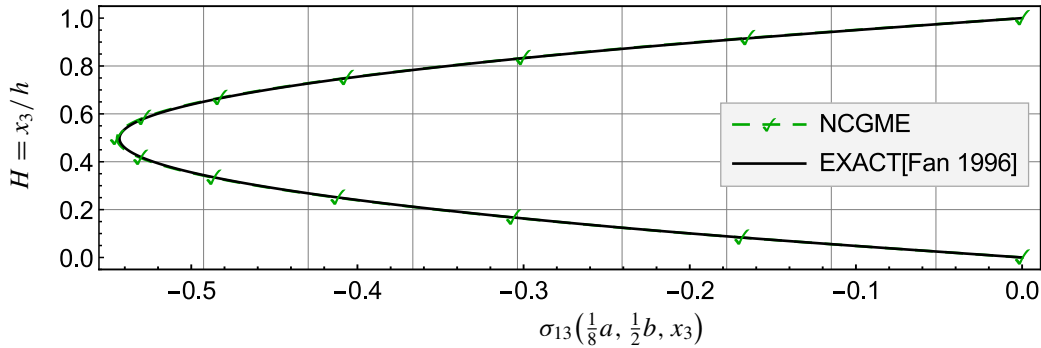
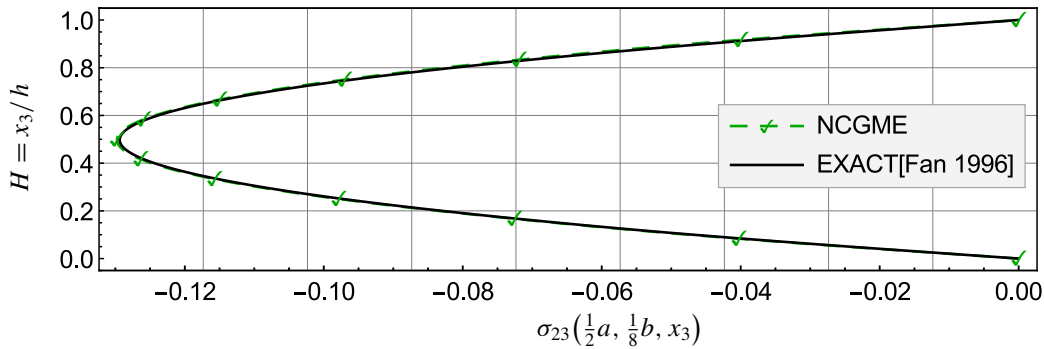


Figure 10. Comparison of stress  $\sigma_{12}(\frac{1}{8}a, \frac{1}{8}b, h)$ .



**Figure 11.** Comparison of stress  $\sigma_{13}(\frac{1}{8}a, \frac{1}{2}b, x_3)$  distribution along thickness of NCGME.



**Figure 12.** Comparison of stress  $\sigma_{23}(\frac{1}{2}a, \frac{1}{8}b, x_3)$  distribution along thickness of NCGME.

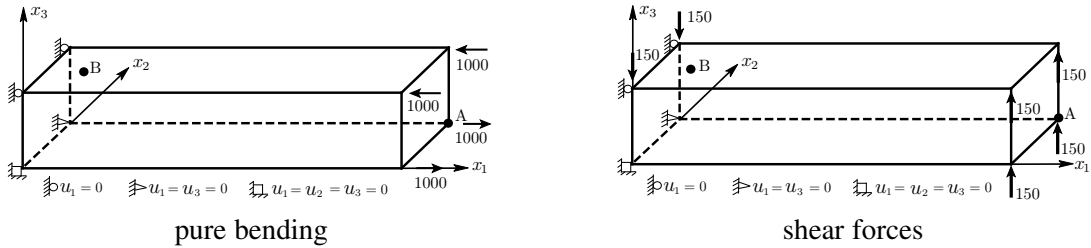
In this example, NCDE can not predict accurately the transversal stresses with respect to the geometrical neutral plane of plate, since the distribution of  $\sigma_{13}$  and  $\sigma_{23}$  along the thickness is nonlinear (see Figures 11 and 12), and the maximum or minimum values on the neutral plane is near to the neutral plane.

Figure 7 indicates that the accuracy of  $\sigma_{33}(\frac{1}{2}a, \frac{1}{2}b, h)$  of NCDE is very poor. As mentioned above, it is difficult to introduce the traction boundary conditions when the stress variables are computed by the constitutive relations (1) on the element level. Hence, the stress results of NCDE on the boundary are inconsistent with the prescribed stresses. However, the stress results of CGMCE8 and NCGMCE8 on the boundary are fully consistent with the prescribed stresses.

The in-plane stress  $\sigma_{22}(\frac{1}{2}a, \frac{1}{2}b, 0)$  of NCGME is characterized by rapid convergence. The accuracy of  $\sigma_{11}(\frac{1}{2}a, \frac{1}{2}b, 0)$ ,  $\sigma_{22}(\frac{1}{2}a, \frac{1}{2}b, 0)$  and  $\sigma_{12}(\frac{1}{8}a, \frac{1}{8}b, h)$  of NCGME is slightly better than NCDE (see Figures 8–10).

On the basis of the mesh  $12 \times 12 \times 4$ , the distribution of both  $\sigma_{13}(\frac{1}{8}a, \frac{1}{2}b, x_3)$  and  $\sigma_{23}(\frac{1}{2}a, \frac{1}{8}b, x_3)$  along the thickness of NCGME are depicted by Figures 11 and 12, respectively. They indicate further that the  $\sigma_{13}$  and  $\sigma_{23}$  can approximate to the exact solutions.

**4.2. A classical cantilever beam problem.** The effect of element geometric distortions on the accuracy of CGME and NCGME are investigated in this example.



**Figure 13.** A cantilever beam under pure bending or acted upon by shear forces at the tip [Cheung and Chen 1988].

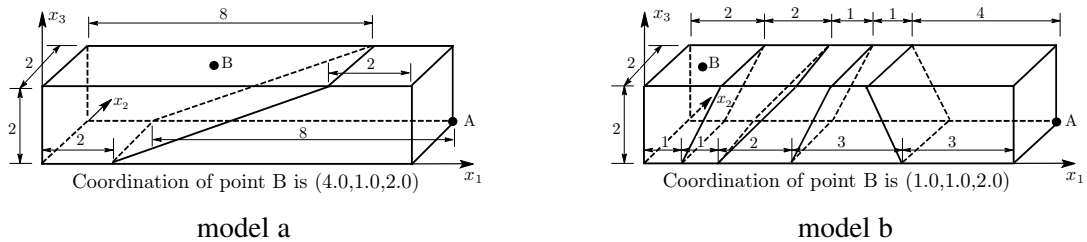


**Figure 14.** Models of element geometric distortion.

load cases	$Q_{S_{11-1}}$	$Q_{S_{11-2}}$	CGME	NCGME	exact
pure bending	31.2	37.5	15.0	75.1	100.0
shear forces	37.4	45.1	22.6	81.8	102.6

**Table 1.** Vertical displacements  $u_3$  at point A of model a.

load cases	$Q_{S_{11-1}}$	$Q_{S_{11-2}}$	CGME	NCGME	exact
pure bending	-1162.4	-1350.9	-423.8	-2549.1	-3000.0
shear forces	-1623.2	-1953.6	-573.3	-2642.9	-2700.0

**Table 2.** The stresses  $\sigma_{11}$  at point B(4.0,1.0,2.0) of model a

Consider a cantilever beam [Cheung and Chen 1988] under pure bending or acted upon by shear forces at the tip (see Figure 13). The geometry dimensions are  $2 \times 2 \times 10$ , and the material properties are  $E = 1500$  and  $\nu = 0.25$ . The vertical displacements at point A and the bending stress  $\sigma_{11}$  at point B for two finite element models (as shown in Figure 14) are presented in Tables 1–4, and they are compared with  $Q_{S_{11-1}}$  [Cheung and Chen 1988],  $Q_{S_{11-2}}$  [Cheung and Chen 1988] and the exact solutions.

From the results listed in Tables 1–4, it can be concluded that:

- (1) The displacement and stress results of NCGME appear to be more accurate than those of the hybrid stress elements  $Q_{S_{11-1}}$  and  $Q_{S_{11-2}}$ .

load cases	$Q_{S_{11-1}}$	$Q_{S_{11-2}}$	CGME	NCGME	exact
pure bending	92.2	92.9	22.7	99.6	100.0
shear forces	94.05	94.9	67.6	103.6	102.6

**Table 3.** Vertical displacements  $u_3$  at point A of model b.

load cases	$Q_{S_{11-1}}$	$Q_{S_{11-2}}$	CGME	NCGME	exact
pure bending	-3006.6	-3015.1	-2294.9	-2996.5	-3000.0
shear forces	-4125.3	-4138.2	-3155.8	-4076.2	-4050.0

**Table 4.** The stresses  $\sigma_{11}$  at point B(1.0,1.0,2.0) of model b.

- (2) Obviously, NCGME is less sensitive to geometric distortions (see Figure 14) in cases where elements are distorted. It is also observed that the accuracy of  $u_3$  and  $\sigma_{11}$  from CGME is very poor due to the geometric distortions of elements.

### 5. Conclusions

For the generalized mixed finite elements presented in this work, both conditions of displacement continuity and traction reciprocity at interelement boundaries are relaxed by including them in the generalized mixed variational principle itself. Hence, the generalized H–R mixed variational principle is crucial to ensure that the generalized mixed elements are effective in obtaining the displacements and stresses directly in the mixed finite element computations. As mentioned in Section 3, two of the most prominent advantages of the compatible and noncompatible generalized mixed elements are that the symmetry with respect to both displacement and stress variables are guaranteed, and the coefficient matrix is invertible. The generalized mixed models seem to be preferable for introducing the displacement and traction boundary conditions simultaneously. The numerical results of the compatible and noncompatible generalized mixed elements are stable and the displacement and stress results of noncompatible generalized mixed elements are characterized by high-precision.

Certainly, like in the traditional mixed methods, a drawback of the generalized mixed methods is a larger number of unknown parameters in the linear system of equations for the finite element analysis. The added number of stress variables means that generally larger size algebraic problems have to be handled. But with the present computer technologies, it is not a problem. In fact, the power of the present computers will always be suitable for a large-scale finite element system. We emphasize that conveniently obtaining stable and highly accurate numerical results is the first priority for the design of engineering structures.

We believe the generalized mixed methods are simple and will be useful, especially as the methods are developed further. For wide engineering structures, some important applications of the noncompatible generalized mixed method should be extended, such as the treatment of the combination with other structural members, the evolution of the possible advantages in stress singularity problems, and nonlinear applications which may result from special structures. The pertinent theories of the generalized mixed elements should also be explored deeply; for instance, investigations of the local error bounds or practical

estimates for the variables should be done. On the other hand, the stresses and the displacements are interpolated with the same interpolation order in this work. Does this choice of interpolation order satisfy the inf-sup Ladyzhenskaya–Babuška–Brezzi (LBB) condition? This work should be discussed in the next paper.

The task of developing high-performance finite element methods for complex engineering problems never seems to be completed.

### Acknowledgments

Authors would like to express their thanks to reviewer for their valuable comments. This work was supported by the Natural Science Foundations of China (11502286).

### References

- [Adams and Cockburn 2005] S. Adams and B. Cockburn, “A mixed finite element method for elasticity in three dimensions”, *J. Sci. Comput.* **25**:3 (2005), 515–521.
- [Arnold 1990] D. N. Arnold, “Mixed finite element methods for elliptic problems”, *Comput. Methods Appl. Mech. Eng.* **82**:1-3 (1990), 281–300.
- [Arnold 2002] D. N. Arnold, “Differential complexes and numerical stability”, pp. 137–157 in *Proceedings of the international congress of mathematicians (ICM 2002), I: Plenary lectures and ceremonies* (Beijing, 2002), Higher Education Press, Beijing, 2002.
- [Arnold and Winther 2002] D. N. Arnold and R. Winther, “Mixed finite elements for elasticity”, *Numer. Math.* **92**:3 (2002), 401–419.
- [Arnold et al. 2007] D. N. Arnold, R. S. Falk, and R. Winther, “Mixed finite element methods for linear elasticity with weakly imposed symmetry”, *Math. Comput.* **76**:260 (2007), 1699–1723.
- [Arnold et al. 2008] D. N. Arnold, G. Awanou, and R. Winther, “Finite elements for symmetric tensors in three dimensions”, *Math. Comput.* **77**:263 (2008), 1229–1251.
- [Atluri et al. 1983] S. N. Atluri, R. H. Gallagher, and O. C. Zienkiewicz, *Hybrid and mixed finite element methods*, Wiley, Chichester, England, 1983.
- [Babuška et al. 1977] I. Babuška, J. T. Oden, and J. K. Lee, “Mixed-hybrid finite element approximations of second-order elliptic boundary-value problems”, *Comput. Methods Appl. Mech. Eng.* **11**:2 (1977), 175–206.
- [Belytschko et al. 2013] T. Belytschko, W. K. Liu, and B. Moran, *Nonlinear finite elements for continua and structures*, 2nd ed., Wiley, Chichester, England, 2013.
- [Bonet and Wood 1997] J. Bonet and R. D. Wood, *Nonlinear continuum mechanics for finite element analysis*, Cambridge University Press, 1997.
- [Brezzi 1974] F. Brezzi, “On the existence, uniqueness and approximation of saddle-point problems arising from Lagrangian multipliers”, *Rev. Française Automat. Informat. Recherche Opérationnelle Sér. Rouge* **8**:R-2 (1974), 129–151.
- [Brezzi and Fortin 1991] F. Brezzi and M. Fortin, *Mixed and hybrid finite element methods*, Springer Series in Computational Mathematics **15**, Springer, New York, 1991.
- [Chen 1982] W. J. Chen, “A high precision eight-node hexahedron element”, *Chin. J. Theor. Appl. Mech.* **3**:26 (1982), 262–271.
- [Cheung and Chen 1988] Y. K. Cheung and W. Chen, “Isoparametric hybrid hexahedral elements for three dimensional stress analysis”, *Int. J. Numer. Methods Eng.* **26**:3 (1988), 677–693.
- [Chien 1983] W. Z. Chien, “Method of high-order Lagrange multiplier and generalized variational principles of elasticity with more general forms of functionals”, *Appl. Math. Mech.* **4**:2 (1983), 143–157.
- [Dunham and Pister 1968] R. S. Dunham and K. S. Pister, “A finite element application of the Hellinger–Reissner variational theorem”, DTIC Document, 1968, <http://oai.dtic.mil/oai/oai?verb=getRecord&metadataPrefix=html&identifier=ADA446774>.

- [Fan 1996] J. R. Fan, *Exact theory of laminated thick plates and shells*, Science Press, Beijing, 1996. In Chinese.
- [Felippa 1989a] C. A. Felippa, “Parametrized multifield variational principles in elasticity, I: Mixed functionals”, *Comm. Appl. Numer. Methods* **5:2** (1989), 79–88.
- [Felippa 1989b] C. A. Felippa, “Parametrized multifield variational principles in elasticity, II: Hybrid functionals and the free formulation”, *Comm. Appl. Numer. Methods* **5:2** (1989), 89–98.
- [Gatica et al. 2008] G. N. Gatica, A. Márquez, and S. Meddahi, “A new dual-mixed finite element method for the plane linear elasticity problem with pure traction boundary conditions”, *Comput. Methods Appl. Mech. Eng.* **197:9-12** (2008), 1115–1130.
- [Gopalakrishnan and Guzmán 2011] J. Gopalakrishnan and J. Guzmán, “Symmetric nonconforming mixed finite elements for linear elasticity”, *SIAM J. Numer. Anal.* **49:4** (2011), 1504–1520.
- [Herrmann 1967] L. R. Herrmann, “Finite element bending analysis for plates”, *J. Eng. Mech. Div. (ASCE)* **93:5** (1967), 13–26.
- [Hoa and Feng 1998] S. V. Hoa and W. Feng, *Hybrid finite element method for stress analysis of laminated composites*, Kluwer Academic Publishers, Boston, 1998.
- [Hu et al. 2016] J. Hu, H. Man, J. Wang, and S. Zhang, “The simplest nonconforming mixed finite element method for linear elasticity in the symmetric formulation on  $n$ -rectangular grids”, *Comput. Math. Appl.* **71:7** (2016), 1317–1336.
- [Morley 1989] M. E. Morley, “A family of mixed finite elements for linear elasticity”, *Numer. Math.* **55:6** (1989), 633–666.
- [Oden 1973] J. T. Oden, “Some contributions to the mathematical theory of mixed finite element approximations”, pp. 3–23 in *Theory and practice in finite element structural analysis: proceedings of the 1973 Tokyo seminar on finite element analysis*, 1973.
- [Oden and Reddy 1976] J. T. Oden and J. N. Reddy, “On mixed finite element approximations”, *SIAM J. Numer. Anal.* **13:3** (1976), 393–404.
- [Pian 1964] T. H. Pian, “Derivation of element stiffness matrices by assumed stress distributions”, *AIAA J.* **2:7** (1964), 1333–1336.
- [Qiu and Demkowicz 2010] W. Qiu and L. Demkowicz, “Variable Order Mixed H-Finite Element Method for Linear Elasticity with Weakly Imposed Symmetry. Ii. Affine and Curvilinear Elements in 2D”, preprint, 2010. arXiv
- [Qiu and Demkowicz 2011] W. Qiu and L. Demkowicz, “Mixed variable order  $h$ -finite element method for linear elasticity with weakly imposed symmetry: curvilinear elements in 2D”, *Comput. Methods Appl. Math.* **11:4** (2011), 510–539.
- [Reissner 1950] E. Reissner, “On a variational theorem in elasticity”, *J. Math. Physics* **29** (1950), 90–95.
- [Sinwel 2009] A. Sinwel, *A new family of mixed finite elements for elasticity*, Ph.D. Thesis, Johannes Kepler University, 2009, <http://www.uni-linz.ac.at>.
- [Talaslidis 1979] D. Talaslidis, “On the convergence of a mixed finite element approximation for cylindrical shells”, *Z. Angew. Math. Mech.* **59:9** (1979), 431–436.
- [Taylor et al. 1976] R. L. Taylor, P. J. Beresford, and E. L. Wilson, “A non-conforming element for stress analysis”, *Int. J. Numer. Methods Eng.* **10:6** (1976), 1211–1219.
- [Tian and Pian 2011] S. Z. Tian and T. H. Pian, *Variational principles with multi-variables and finite element methods with multi-variables*, Science Press, Beijing, 2011. In Chinese.
- [Zienkiewicz and Taylor 2000] O. C. Zienkiewicz and R. L. Taylor, *The finite element method, II: Solid mechanics*, 5th ed., Butterworth-Heinemann, Oxford, 2000.

Received 2 Feb 2017. Revised 20 Mar 2017. Accepted 25 Apr 2017.

GUANGHUI QING: [qingluke@126.com](mailto:qingluke@126.com)

College of Aeronautical Engineering, Civil Aviation University of China, Jinbei Road 2898, Tianjin, 300300, China

JUNHUI MAO: [maojunhui@outlook.com](mailto:maojunhui@outlook.com)

College of Aeronautical Engineering, Civil Aviation University of China, Jinbei Road 2898, Tianjin, 300300, China

YANHONG LIU: [lyhqzh@126.com](mailto:lyhqzh@126.com)

College of Aeronautical Engineering, Civil Aviation University of China, Jinbei Road 2898, Tianjin, 300300, China



# JOURNAL OF MECHANICS OF MATERIALS AND STRUCTURES

[msp.org/jomms](http://msp.org/jomms)

Founded by Charles R. Steele and Marie-Louise Steele

## EDITORIAL BOARD

ADAIR R. AGUIAR	University of São Paulo at São Carlos, Brazil
KATIA BERTOLDI	Harvard University, USA
DAVIDE BIGONI	University of Trento, Italy
YIBIN FU	Keele University, UK
IWONA JASIUK	University of Illinois at Urbana-Champaign, USA
MITSUTOSHI KURODA	Yamagata University, Japan
C. W. LIM	City University of Hong Kong
THOMAS J. PENCE	Michigan State University, USA
GIANNI ROYER-CARFAGNI	Università degli studi di Parma, Italy
DAVID STEIGMANN	University of California at Berkeley, USA
PAUL STEINMANN	Friedrich-Alexander-Universität Erlangen-Nürnberg, Germany

## ADVISORY BOARD

J. P. CARTER	University of Sydney, Australia
D. H. HODGES	Georgia Institute of Technology, USA
J. HUTCHINSON	Harvard University, USA
D. PAMPLONA	Universidade Católica do Rio de Janeiro, Brazil
M. B. RUBIN	Technion, Haifa, Israel

**PRODUCTION** [production@msp.org](mailto:production@msp.org)

SILVIO LEVY Scientific Editor

Cover photo: Mando Gomez, [www.mandolux.com](http://www.mandolux.com)

---

See [msp.org/jomms](http://msp.org/jomms) for submission guidelines.

---

JoMMS (ISSN 1559-3959) at Mathematical Sciences Publishers, 798 Evans Hall #6840, c/o University of California, Berkeley, CA 94720-3840, is published in 10 issues a year. The subscription price for 2017 is US \$615/year for the electronic version, and \$775/year (+\$60, if shipping outside the US) for print and electronic. Subscriptions, requests for back issues, and changes of address should be sent to MSP.

---

JoMMS peer-review and production is managed by EditFLOW<sup>®</sup> from Mathematical Sciences Publishers.

PUBLISHED BY

 **mathematical sciences publishers**  
nonprofit scientific publishing

<http://msp.org/>

© 2017 Mathematical Sciences Publishers

# Journal of Mechanics of Materials and Structures

Volume 12, No. 4

July 2017

---

<b>B-splines collocation for plate bending eigenanalysis</b>	<b>CHRISTOPHER G. PROVATIDIS</b>	<b>353</b>
<b>Shear capacity of T-shaped diaphragm-through joints of CFST columns</b>	<b>BIN RONG, RUI LIU, RUOYU ZHANG, SHUAI LIU and APOSTOLOS FAFITIS</b>	<b>373</b>
<b>Polarization approximations for elastic moduli of isotropic multicomponent materials</b>	<b>DUC CHINH PHAM, NGUYEN QUYET TRAN and ANH BINH TRAN</b>	<b>391</b>
<b>A nonlinear micromechanical model for progressive damage of vertebral trabecular bones</b>	<b>EYASS MASSARWA, JACOB ABOUDI, FABIO GALBUSERA, HANS-JOACHIM WILKE and RAMI HAJ-ALI</b>	<b>407</b>
<b>Nonlocal problems with local Dirichlet and Neumann boundary conditions</b>	<b>BURAK AKSOYLU and FATIH CELIKER</b>	<b>425</b>
<b>Optimization of Chaboche kinematic hardening parameters by using an algebraic method based on integral equations</b>	<b>LIU SHIJIE and LIANG GUOZHU</b>	<b>439</b>
<b>Interfacial waves in an A/B/A piezoelectric structure with electro-mechanical imperfect interfaces</b>	<b>M. A. REYES, J. A. OTERO and R. PÉREZ-ÁLVAREZ</b>	<b>457</b>
<b>Fully periodic RVEs for technological relevant composites: not worth the effort!</b>	<b>KONRAD SCHNEIDER, BENJAMIN KLUSEMANN and SWANTJE BARGMANN</b>	<b>471</b>
<b>Homogenization of a Vierendeel girder with elastic joints into an equivalent polar beam</b>	<b>ANTONIO GESUALDO, ANTONINO IANNUZZO, FRANCESCO PENTA and GIOVANNI PIO PUCILLO</b>	<b>485</b>
<b>Highly accurate noncompatible generalized mixed finite element method for 3D elasticity problems</b>	<b>GUANGHUI QING, JUNHUI MAO and YANHONG LIU</b>	<b>505</b>
<b>Thickness effects in the free vibration of laminated magneto-electroelastic plates</b>	<b>CHAO JIANG and PAUL R. HEYLIGER</b>	<b>521</b>
<b>Localized bulging of rotating elastic cylinders and tubes</b>	<b>JUAN WANG, ALI ALTHOBAITI and YIBIN FU</b>	<b>545</b>



1559-3959(2017)12:4;1-1